

Elementary formulae for social distancing scenarios: Application to COVID-19 mitigation via feedback control

Michel Fliess^{1,3} and Cédric Join^{2,3}

Abstract

Social distancing has been enacted in order to mitigate the spread of COVID-19. Like many authors, we adopt the classic epidemic SIR model, where the infection rate is the control variable. Its differential flatness property yields elementary closed-form formulae for open-loop social distancing scenarios, where, for instance, the increase of the number of uninfected people may be taken into account. Those formulae might therefore be useful to decision makers. A feedback loop stemming from model-free control leads to a remarkable robustness with respect to severe uncertainties of various kinds. Although an identification procedure is presented, a good knowledge of the recovery rate is not necessary for our control strategy. Several convincing computer experiments are displayed.

Index Terms

Biomedical control, COVID-19, social distancing, SIR model, nonlinear feedback control, flatness-based control, model-free control, robustness, identifiability, algebraic differentiator

arXiv:2110.01712v1 [eess.SY] 4 Oct 2021

¹LIX (CNRS, UMR 7161), École polytechnique, 91128 Palaiseau, France. Michel.Fliess@polytechnique.edu

²CRAN (CNRS, UMR 7039), Université de Lorraine, BP 239, 54506 Vandœuvre-lès-Nancy, France. cedric.join@univ-lorraine.fr

³AL.I.E.N., 7 rue Maurice Barrès, 54330 Vézelize, France. {michel.fliess, cedric.join}@alien-sas.com

I. INTRODUCTION

In less than two years an abundant mathematically oriented literature has been devoted to the worldwide COVID-19 pandemic. Some of the corresponding calculations had even a significant political impact (see, *e.g.*, [1]). A novel control technique for improving the social distancing is presented here. This fundamental topic has already been tackled by many authors: see, *e.g.*, [2], [3], [6], [7], [8], [10], [12], [13], [14], [15], [21], [25], [30], [28], [36], [37], [38], [41], [43], [44], [46], [57]. Most of those papers are based on the famous *SIR* (*Susceptible-Infected-Recovered/Removed*) model, which goes back to [27] in 1927, or on slight modifications. This communication is also using the SIR model:

- When, like in several papers, the *infection rate* is the control variable, the SIR model is (*differentially flat*) ([20]). Remember that flatness-based control is one of the most popular model-based control setting, especially with respect to concrete applications: see, *e.g.*, [5], [9], [31], [32], [35], [45], [47], [49], [50], [51], [53], [54], [55], [63] for some recent publications. Note that flatness has already been utilized in [23] for studying COVID-19 but with other purposes.
- There are severe uncertainties: model mismatch, poorly known initial conditions, ... We therefore close the loop around the reference trajectory via *model-free* control, or *MFC*, in the sense of [16], [17]. MFC, which is easy to implement, has already been illustrated in a number of practical situations. Some new contributions are listed here: [22], [26], [29], [33], [39], [40], [48], [52], [58], [59], [60], [61], [64], [65]. Let us single out here the excellent work by [56] on ventilators, which are obviously related to COVID-19.

In order to be more specific consider a flat system with a single input u and a single output y . Assume that y is a flat output. Our strategy may be summarized as follows:

- 1) To any output reference trajectory y^* corresponds at once thanks to flatness an open-loop control u^* .
- 2) Let z be some measured output. Write z^* the corresponding reference trajectory. Set $u = u^* + \Delta u$, where Δu is the control of an *ultra-local* local model [16]. Its output $\Delta z = z - z^*$ is the tracking error. Closing the loop via an *intelligent controller* [16] permits to ensure local stability around z^* in spite of severe mismatches and disturbances.

Our paper is organized as follows.

- Section II shows that
 - the SIR model, where the infection rate is the control variable, is flat and the population of recovered/removed individuals is a flat output;
 - the recovery rate is identifiable in the sense of [19].
- Section III is devoted to a flatness-based control strategy, *i.e.*, to a feedforward approach. Elementary closed-form of the control and state variables are easily derived. Various scenarios, where for instance the number of uninfected persons is increased, may thus be easily suggested to decision makers.
- Closing the loop via an intelligent proportional regulator, stemming from model-free control, is the subject of Section IV. Computer simulations confirm an excellent robustness with respect to severe uncertainties.
- A time-varying recovery rate is estimated in Section V via *algebraic estimation* methods ([19]). Techniques from Section IV show however good performances if this rate is wrongly assumed to be constant.
- Some concluding remarks may be found in Section VI.

II. MODELING ISSUES

A. The SIR model

The SIR model (see, *e.g.*, [62] for a most pleasant introduction) reads:

$$\begin{cases} \dot{S} = -\beta IS \\ \dot{I} = \beta IS - \gamma I \\ \dot{R} = \gamma I \end{cases} \quad (1)$$

S , I and R , which are non-negative quantities, correspond respectively to the fractions of susceptible, infected and recovered/removed individuals in the population. We may set therefore

$$S + I + R = 1 \quad (2)$$

β , $0 < \underline{\beta} \leq \beta \leq \bar{\beta}$, which is here the control variable,¹ and the constant parameter $\gamma > 0$ are the infection and recovery rates.

B. Flatness

Equations (1)-(2) show that System (1) is flat and that R is a flat output [20]. The other system variables may be expressed as *differential rational functions* of R , *i.e.*, as rational functions of R and its derivatives up to some finite order:

$$I = \frac{\dot{R}}{\gamma} \quad (3)$$

$$S = 1 - R - \frac{\dot{R}}{\gamma} \quad (4)$$

$$\beta = -\frac{\dot{S}}{IS} = \frac{1}{S} \left(\frac{\dot{I}}{I} + \gamma \right) \quad (5)$$

Remark 1: If γ is not constant, but a differentiable function of time, Equations (3)-(4)-(5) remain valid: System (1) is still flat and R is still a flat output. Equation (5) shows however that $\dot{\gamma}$ is needed.

¹Softening social distancing implies increasing $\beta(t)$.

C. Identifiability of the recovery rate

Equation (5) yields

$$\gamma = \beta S - \frac{\dot{I}}{I}$$

γ is a differential rational function of R and β : It is thus *rationally identifiable* [19].

Remark 2: The above equation does not work for an identifiability purpose if γ is time-varying: $\dot{\gamma}$ is sitting on its right hand-side. If we assume that I and S are measured, Equation (4) yields

$$\gamma = \frac{\dot{I} - \beta IS}{I} \quad (6)$$

γ is still rationally identifiable with respect to I, S, β . It will be useful in Section V.

III. FLATNESS-BASED CONTROL

A. Preparatory calculations

Set

$$I_{\text{reference}}(t) = I_0 e^{-\lambda t}$$

where $t \geq 0$, $0 \leq I_0 \leq 1$, and $\lambda \geq 0$ is some constant parameter.

Remark 3: The *reproduction number* (see, e.g., [24], [62]) is thus set to $\exp(-\lambda) < 1$. If we set $R(0) = 0$, it yields

$$R_{\text{reference}}(t) = \frac{\gamma I_0}{\lambda} (1 - e^{-\lambda t})$$

$$S_{\text{reference}}(t) = 1 - \frac{\gamma I_0}{\lambda} (1 - e^{-\lambda t}) - I_0 e^{-\lambda t}$$

and the open-loop control

$$\beta_{\text{flat}}(t) = \frac{\gamma - \lambda}{1 - \frac{\gamma I_0}{\lambda} (1 - e^{-\lambda t}) - I_0 e^{-\lambda t}}$$

Thus

$$\lim_{t \rightarrow +\infty} \beta_{\text{flat}}(t) = \frac{\lambda(\gamma - \lambda)}{\lambda - \gamma I_0} \quad (7)$$

The following inequalities are straightforward:

$$\gamma I_0 < \lambda < \gamma \quad (8)$$

$\lambda < \gamma$ follows from $\beta > 0$; $\gamma I_0 < \lambda$ follows from

$$\lim_{t \rightarrow +\infty} S(t) = 1 - \frac{\gamma I_0}{\lambda} = S(\infty) > 0 \quad (9)$$

Introduce the more or less precise quantity β_{accept} , where $\beta < \beta_{\text{accept}} < \bar{\beta}$. It stands for the ‘‘harsh’’ social distancing protocols which are ‘‘acceptable’’ in the long run. Equation (7) yields therefore

$$\frac{\lambda(\gamma - \lambda)}{\lambda - \gamma I_0} = \beta_{\text{accept}}$$

The positive root of the corresponding quadratic algebraic equation $\lambda^2 + (\beta_{\text{accept}} - \gamma)\lambda - \gamma I_0 \beta_{\text{accept}} = 0$ is

$$\lambda_{\text{accept}} = \frac{\gamma - \beta_{\text{accept}} + \sqrt{\Delta_{\text{accept}}}}{2}$$

where $\Delta_{\text{accept}} = (\gamma - \beta_{\text{accept}})^2 + 4\gamma I_0 \beta_{\text{accept}} \geq 0$. The fundamental inequality

$$\gamma I_0 < \lambda_{\text{accept}} < \gamma$$

follows from

$$\lim_{\lambda \downarrow \gamma I_0} \frac{\lambda(\gamma - \lambda)}{\lambda - \gamma I_0} = +\infty, \quad \lim_{\lambda \uparrow \gamma} \frac{\lambda(\gamma - \lambda)}{\lambda - \gamma I_0} = 0$$

Equation (9) leads to the notation

$$S_{\text{accept}}(\infty) = 1 - \frac{\gamma I_0}{\lambda_{\text{accept}}}$$

The inequality

$$S(\infty) < S_{\text{accept}}(\infty) \quad \text{if} \quad \lambda < \lambda_{\text{accept}}$$

demonstrates that the proportion of uninfected people decreases if the social distancing obligations are relaxed.

B. Two computer experiments

Set $\gamma = 0.1$, $\beta_{\text{accept}} = 0.22$. Figure 1 displays the open-loop evolutions of β , I , S when $\lambda = \lambda_{\text{accept}}$. Those behaviors are quite satisfactory.

IV. MODEL-FREE CONTROL

A. Ultra-local model

Set $\Delta I(t) = I(t) - I_{\text{reference}}(t)$, $\beta(t) = \beta_{\text{flat}}(t) + \Delta\beta(t)$. In order to take into account the various uncertainties, introduce the *ultra-local* model ([16])

$$\frac{d}{dt}\Delta I = F + \alpha\Delta\beta \quad (10)$$

- The function F , which is data-driven, subsumes the poorly known structures and disturbances.
- The parameter α , which does not need to be precisely determined, is chosen such that the three terms in Equation (10) are of the same magnitude.
- $F_{\text{est}} = -\frac{6}{\tau^3} \int_{t-\tau}^t ((t-2\sigma)\Delta I(\sigma) + \alpha\sigma(\tau-\sigma)\Delta\beta(\sigma)) d\sigma$, where $\tau > 0$ is “small”, gives a real-time estimate, which in practice is implemented via a digital filter.

B. Intelligent proportional controller

Introduce ([16]) the *intelligent proportional controller*, or *iP*,

$$\Delta\beta = -\frac{F_{\text{est}} + K_P\Delta I}{\alpha} \quad (11)$$

where K_P is a tuning gain. Equations (10) and (11) yield

$$\frac{d}{dt}\Delta I + K_P\Delta I = F - F_{\text{est}}$$

Set $K_P > 0$. Then $\lim_{t \rightarrow +\infty} \Delta I(t) \approx 0$ if the estimate F_{est} is “good,” *i.e.*, if $F - F_{\text{est}}$ is “small.” Local stability is ensured.

Remark 4: When compared to classic PIs and PIDs (see, *e.g.*, [4]), the gain tuning of the *iP* is straightforward.

C. Computer experiments

The sampling time interval is 2 hours. In Equations (10) and (11), $\alpha = 0.1$, $K_P = 1$. Figure 2 displays excellent results in spite of

- errors on initial conditions;
- the fuzzy character of any measurement of the social distancing. It is expressed by an additive corrupting white Gaussian noise $\mathcal{N}(0, 5 \cdot 10^{-3})$ on β .

V. ON THE RECOVERY RATE γ

Assume now that γ is a differentiable time function. Equation (6) yields the algebraic estimator

$$\gamma_{\text{est}} = \frac{[\dot{I}]_{\text{est}} - \beta IS}{I} \quad (12)$$

where $[\dot{I}]_{\text{est}}$ is an estimate of \dot{I} obtained along the lines developed in [34], [42] for *algebraic differentiators*. Figure 3-c displays excellent results. The flatness-based computer experiments is achieved as in Section III-B, *i.e.*, $\gamma = 0.1$ is assumed to be constant. Lack of space prevents us from displaying our convincing simulations in the more realistic situation with noise corruption.

Closing the loop via model-free control yields as demonstrated in Figures 3-a-b a rather satisfactory behavior. Should we deduce that the exact knowledge of the recovery rate is unimportant?

VI. CONCLUSION

The relevance and usefulness of such control-theoretic considerations for non-pharmaceutical mitigation policies against COVID-19 are questioned in [11]. We certainly do not claim to set aside those objections in this preliminary short study. The combination however of flatness-based and model-free controls, like in [18] for *in silico* cancer treatments, presents perhaps some major advantages:

- Flatness-based control allows to present in a straightforward way a wealth of reference trajectories in order to take into account various constraints.
- Closing the loop via model-free control permits a remarkable robustness with respect to many severe uncertainties.

Those features should of course be confirmed by further investigations.

REFERENCES

- [1] Adam D. (2020). Special report: the simulations driving the world's response to COVID-19. *Nature*, 580, 316-318.
- [2] Ames A.Z., Molnár T.G., Singletary A.W., Orosz G. (2020). Safety-critical control of active interventions for COVID-19 mitigation. *IEEE Access*, 8, 188454-188474.
- [3] Angulo M.T., Castañón F., Moreno-Morton R., Velasco-Hernández J.X., Moreno J.A. (2021). A simple criterion to design optimal non-pharmaceutical interventions for mitigating epidemic outbreaks. *J. Roy. Soc. Interface*, 18, 20200803.
- [4] Åström K.J., Murray R.M. (2008). *Feedback Systems: An Introduction for Scientists and Engineers*. Princeton University Press.
- [5] Beltran-Carbajal F., Tapia-Olvera R., Valderrabano-Gonzalez A., Yanez-Badillo H., Rosas-Caro J.C., Mayo-Maldonado J.C. (2021). Closed-loop online harmonic vibration estimation in DC electric motor systems. *Appl. Math. Model.*, 94, 460-481.
- [6] Bisiacco M., Pillonetto G. (2021). COVID-19 epidemic control using short-term lockdowns for collective gain. [arXiv:2109.00995](https://arxiv.org/abs/2109.00995)
- [7] Bliman P.-A., Duprez M. (2021). How best can finite-time social distancing reduce epidemic final size? *J. Theoret. Biol.*, 511, 110557.
- [8] Bliman P.-A., Duprez M., Privat Y., Vauchelet N. (2021). Optimal immunity control and final size minimization by social distancing for the SIR epidemic model. *J. Optim. Theory App.*, 189, 408-436.
- [9] Bonnabel S., Clayes X. (2020). The industrial control of tower cranes: An operator-in-the-loop approach. *IEEE Contr. Syst. Magaz.*, 40, 27-39.
- [10] Borri A., Palumbo P., Papa F., Possieri C. (2021). Optimal design of lock-down and reopening policies for early-stage epidemics through SIR-D models *Annual Rev. Contr.* 51, 511-524.
- [11] Casella F. (2021). Can the COVID-19 epidemic be controlled on the basis of daily test reports? *IEEE Contr. Syst. Lett.*, 5, 1079-1084.
- [12] Charpentier A., Elie R., Laurière M., Tran V.C. (2020). COVID-19 pandemic control: balancing detection policy and lockdown intervention ICU sustainability. *Math. Model. Nat. Phenom.*, 15, 57.
- [13] Di Lauro F., Kiss I.Z., Della Santina C. (2021). Optimal timing of one-shot interventions for epidemic control. *PLoS Comput. Biol.*, 17, e1008763.
- [14] Di Lauro F., Kiss I.Z., Della Santina C. (2021). Covid-19 and flattening the curve: A feedback control perspective. *IEEE Contr. Syst. Lett.*, 5, 1435-1440.
- [15] Dias S., Queiroz K., Araujo A. (2021). Controlling epidemic diseases based only on social distancing level. *J. Contr. Autom. Electr. Syst.*, <https://doi.org/10.1007/s40313-021-00745-6>
- [16] Fliess M., Join C. (2013). Model-free control. *Int. J. Contr.*, 86, 2228-2252.
- [17] Fliess M., Join C. (2021). An alternative to proportional-integral and proportional-integral-derivative regulators: Intelligent proportional-derivative regulators. *Int. J. Robust Nonlinear Contr.*, <https://doi.org/10.1002/rnc.5657>
- [18] Fliess M., Join C., Moussa K., Djouadi S.M., Alsager M.W. (2021). Toward simple in silico experiments for drugs administration in some cancer treatments. *11th IFAC Symp. Biolog. Medic. Syst.*, Ghent. <https://hal.archives-ouvertes.fr/hal-03299417/en/>
- [19] Fliess M., Join C., Sira-Ramirez H. (2008). Non-linear estimation is easy. *Int. J. Model. Identif. Contr.*, 4, 12-27.
- [20] Fliess M., Lévine J., Martin P., Rouchon P. (1995). Flatness and defect of non-linear systems: introductory theory and examples. *Int. J. Contr.*, 61, 1327-1361.
- [21] Gevertz J.L., Greene J.M., Sanchez-Tapia C.H., Sontag E.D. (2021). A novel COVID-19 epidemiological model with explicit susceptible and asymptomatic isolation compartments reveals unexpected consequences of timing social distancing. *J. Theoret. Biol.*, 510, 110539.
- [22] Gu J., Li H., Zhang H., Pan C., Luan Z. (2021). Cascaded model-free predictive control for single-phase boost power factor correction converters. *Int. J. Robust Nonlinear Contr.*, 31, 5016-5032.
- [23] Hametner C., Kozek M., Böehler L., Wasserburger A., Peng Du Z., Kölbl R., Bergmann M., Bachleitner-Hofmann T., Jakubek S. (2021). Estimation of exogenous drivers to predict COVID-19 pandemic using a method from nonlinear control theory. *Nonlin. Dyn.*, <https://doi.org/10.1007/s11071-021-06811-7>
- [24] Heesterbeek J.A.P. (2002). A brief history of R_0 and a recipe for its calculation. *Acta Biotheo.*, 50, 189-204.
- [25] Ianni A., Rossi N. (2021). SIR-PID: A proportional-integral-derivative controller for COVID-19 outbreak containment. *Physics*, 3, 459-472.
- [26] Ismail A., Noura H., Harmouch F., Harb Z. (2021). Design and control of a neonatal incubator using model-free control. *29th Medit. Conf. Contr. Automat.*, Puglia.
- [27] Kermack W.O., McKendrick A.G. (1927). A contribution to the mathematical theory of epidemics. *Proc. Royal Soc. London Ser. A*, 115, 700-721.
- [28] Köhler J., Schwenkel L., Koch A., Berberich J., Pauli P., Allgöwer F. (2021). Robust and optimal predictive control of the COVID-19 outbreak. *Annual Rev. Contr.*, 51, 525-539.
- [29] Kuruganti T., Olama M., Dong J., Xue Y., Winstead C., Nutaro J., Djouadi S., Bai L., Augenbroe G., Hill J. (2021). *Dynamic Building Load Control to Facilitate High Penetration of Solar Photovoltaic Generation*. Tech. Rep. ORNL/TM-2021/2112, Oak Ridge National Lab.
- [30] Jing M., Yew Ng K., Mac Namee B., Biglarbeigi P., Brisk R., Bond R., Finlay D., McLaughlin J. (2021). COVID-19 modelling by time-varying transmission rate associated with mobility trend of driving via Apple Maps. *J. Biomed. Informat.*, 122, 103905.
- [31] Li X., Wang Y., Guo X., Cui X., Zhang S., Li Y. (2021). An improved model-free current predictive control method for SPMSM drives. *IEEE Access*, DOI: 10.1109/ACCESS.2021.3115782
- [32] Lorenz-Meyer M.N.L., Menzel R., Dadzis K., Nikiforova A., Riemann H. (2020). Lumped parameter model for silicon crystal growth from granulate crucible. *Cryst. Res. Technol.*, 55, 2000044.
- [33] Mao J., Li H., Yang L., Zhang H., Liu L., Wang X., Tao J. (2021). Non-cascaded model-free predictive speed control of SMPMSM drive system. *IEEE Trans. Energ. Convers.*, doi: 10.1109/TEC.2021.3090427
- [34] Mboup M., Join C., Fliess M. (2009). Numerical differentiation with annihilators in noisy environment. *Numer. Algor.*, 50, 439-467.
- [35] Miuncke T. (2020). *Ein szenarienadaptiver Bewegungsalgorithmus für die Längsbewegung eines vollbeweglichen Fahrsimulators*. Springer.
- [36] Morato M.M., Bastos S.B., Cajueiro D.O., Normey-Rico J.E. (2020). An optimal predictive control strategy for COVID-19 (SARS-CoV-2) social distancing policies in Brazil. *Annual Rev. Contr.*, 50, 417-431.
- [37] Morato M.M., Patato I.M.L., Americano da Costa M.V., Normey-Rico J.E. (2020). A parametrized nonlinear predictive control strategy for relaxing COVID-19 social distancing measures in Brazil. *ISA Trans.*, <https://doi.org/10.1016/j.isatra.2020.12.012>
- [38] Morris D.H., Rossine F.W., Plotkin J.B., Levin S.A. (2021). Optimal, near-optimal, and robust epidemic control. *Communic. Phys.*, 4, 78.
- [39] Mousavi M.S., Davari S.A., Nekoukar V., Garcia C., Rodriguez J. (2021). Model-free finite set predictive voltage control of induction motor. *12th Power Electron. Drive Syst. Techno. Conf.*, Tabriz.
- [40] Neves G., Angélico B.A. (2021). Model-free control of mechatronic systems based on algebraic estimation. *Asian J. Contr.*, <https://doi.org/10.1002/asjc.2596>
- [41] O'Sullivan D., Gahegan M., Daniel J. Exeter D.J., Adams B. (2020). Spatially explicit models for exploring COVID-19 lockdown strategies. *Trans. GIS*, 24, 967-1000.

- [42] Othmane A., Rudolph J., Mounier H. (2021). Systematic comparison of numerical differentiators and an application to model-free control. *Europ. J. Contr.*, <https://doi.org/10.1016/j.ejcon.2021.06.020>
- [43] Péni T., Csutak B., Szederkényi G., Röst G. (2020). Nonlinear model predictive control with logic constraints for COVID-19 management. *Nonlin. Dyn.*, 102, 1965-1986.
- [44] Pillonetto G., Bisiacco M., Palù G., Cobelli C. (2021). Tracking the time course of reproduction number and lockdown's effect on human behaviour during SARS-CoV-2 epidemic: nonparametric estimation. *Sci. Rep.*, 11, 9772.
- [45] Richter H., Warner H. (2021). Motion optimization for musculoskeletal dynamics: A flatness-based polynomial approach. *IEEE Trans. Automat. Contr.*, DOI: 10.1109/TAC.2020.3029318
- [46] Sadeghi M., Greene J.M., Sontag E.D. (2021). Universal features of epidemic models under social distancing guidelines. *Annual Rev. Contr.*, 51, 426-440.
- [47] Sahoo S.R., Chiddarwar S.S. (2020). Flatness-based control scheme for hardware-in-the-loop simulations of omnidirectional mobile robot. *Simul.*, 96, 169-183.
- [48] Sancak C., Yamac F., Itik, M., Alici G. (2021). Force control of electro-active polymer actuators using model-free intelligent control. *J. Intel. Mater. Syst. Struct.*, <https://doi.org/10.1177/1045389X20986992>
- [49] Sanchez J.C., Gavilan F., Vazquez R., Louembet C. (2020). A flatness-based predictive controller for six-degrees of freedom spacecraft rendezvous. *Acta Astronaut.*, 167, 391-403.
- [50] Schörghuber C., Göllés M., Reichhartinger M., Horn M. (2020). Control of biomass grate boilers using internal model control. *Contr. Eng. Pract.*, 96, 104274.
- [51] Steckler P.-B., Gauthier J.-Y., Lin-Shi X., Wallart (2021). Differential flatness-based, full-order nonlinear control of a modular multilevel converter (MMC). *IEEE Trans. Contr. Syst. Technol.*, DOI: 10.1109/TCST.2021.3067887
- [52] Sun J., Wang J., Yang P., Guo S. (2021). Model-free prescribed performance fixed-time control for wearable exoskeletons. *Appl. Math. Model.*, 90, 61-77.
- [53] Tal E.A., Karaman S. (2021). Global trajectory-tracking control for a tailsitter flying wing in agile uncoordinated flight. *AIAA Aviat. Forum.*
- [54] Thounthong P., Mungporn P., Guilbert D., Takorabet N., Pierfederic S., Nahid-Mobarekeh B., Hug Y., Bizouh N., Huangfui Y., Kumamj P. (2021). Design and control of multiphase interleaved boost converters-based on differential flatness theory for PEM fuel cell multi-stack applications. *Elect. Power Ener. Syst.*, 124, 106346.
- [55] Tognon M., Franchi A. (2021). *Theory and Applications for Control of Aerial Robots in Physical Interaction Through Tethers*. Springer.
- [56] Truong C.T., Huynh K.H., Duong V.T., Nguyen H.H., Pham L.A., Nguyen T.T. (2021). Model-free volume and pressure cycled control of automatic bag valve mask ventilator. *AIMS Bioengin.*, 8, 192-207.
- [57] Tsay C., Lejarza F., Stadtherr M.A., Baldea M. (2020). Modeling, state estimation, and optimal control for the US COVID-19 outbreak. *Scientif. Rep.*, 10, 10711.
- [58] Xu L., Chen G., Li Q. (2020). Ultra-local model-free predictive current control based on nonlinear disturbance compensation for permanent magnet synchronous motor. *IEEE Access*, 8, 127690-127699.
- [59] Xu L., Chen G., Li Q. (2021). Cascaded speed and current model of PMSM with ultra-local model-free predictive control. *Int. J. Robust Nonlinear Contr.* <https://doi.org/10.1049/elp2.12108>
- [60] Wang Y., Li H., Liu R., Yang L., Wang X. (2020). Modulated model-free predictive control with minimum switching losses for PMSM drive system. *IEEE Access*, 8, 20942-20953.
- [61] Wang Z., Wang J. (2020). Ultra-local model predictive control: A model-free approach and its application on automated vehicle trajectory tracking. *Contr. Eng. Pract.*, 101, 104482.
- [62] Weiss H. (2013). The SIR model and the foundations of public health. *Materials matemàtics*, <https://ddd.uab.cat/record/108432>
- [63] Zauner M., Mandl P., König O., Hametner C., Jakubek S. (2021). Stability analysis of a flatness-based controller driving a battery emulator with constant power load. *at-Automatisierungstech.*, 69,142-154.
- [64] Zhang Y., Jiang T., Jiao J. (2020). Model-free predictive current control of a DFIG using an ultra-local model for grid synchronization and power regulation. *IEEE Trans. Energ. Conv.*, 35, 2269-2280.
- [65] Zhang Y., Wang X., Yang H., Zhang B., Rodriguez J. (2021). Robust predictive current control of induction motors based on linear extended state observer. *Chinese J. Elec. Engin.*, 7, 94-105.

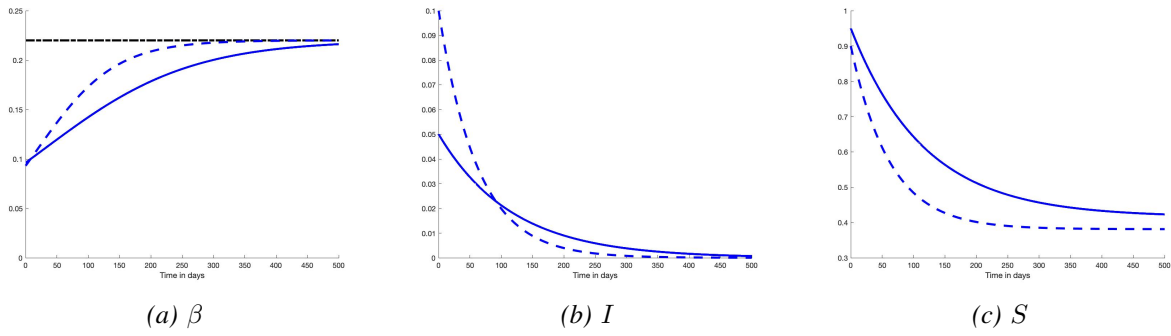


Fig. 1: Open loop: $I_0 = 0.05$ (-) and $I_0 = 0.1$ (- -)

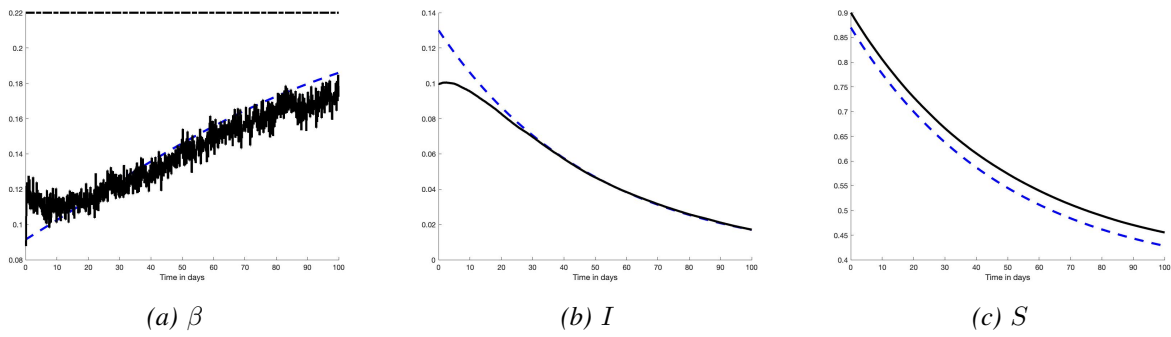
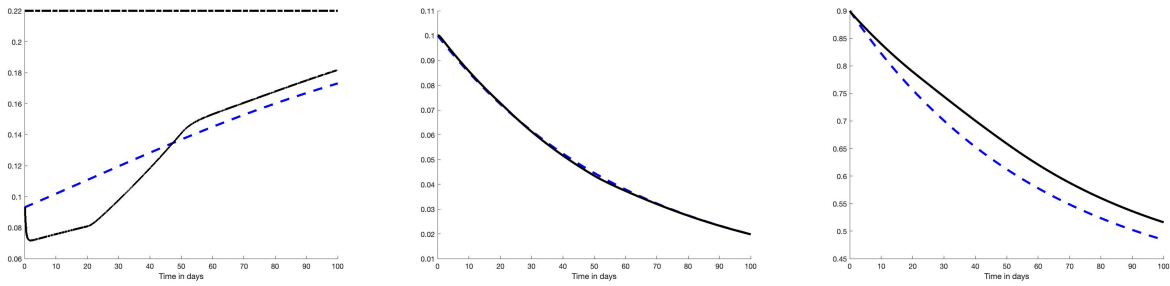
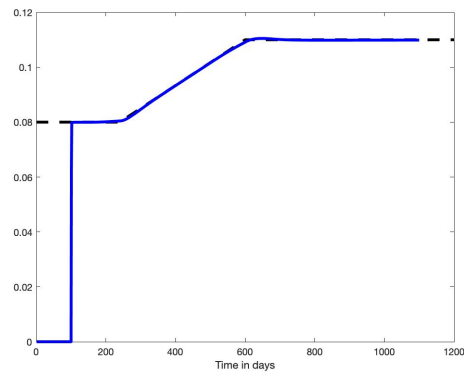


Fig. 2: Error on initial conditions and fuzzy β – blue(- -): reference trajectory



(a) β – blue(- -): reference trajectory (b) I – blue(- -): reference trajectory (c) S – blue(- -): reference trajectory



(d) γ (- -) and γ_{est} (blue -)

Fig. 3: Variable recovery rate γ